

FAST LIGHT ENHANCEMENT BY BIDIRECTIONAL PUMPING IN ERBIUM-DOPED FIBERS

J. M. EZQUERRO*, G. HERNÁNDEZ, M. NOMBELA,
OSCAR G. CALDERÓN and SONIA MELLE

*Escuela Universitaria de Óptica,
Universidad Complutense de Madrid,
C/Arcos de Jalón 118,
28037 Madrid, Spain
josemi@opt.ucm.es

Received 10 February 2010

We analyze the effect of pump configuration on the propagation velocity of an amplitude-modulated 1536 nm signal propagating through an ultra-highly doped erbium fiber amplifier. The nonlinear effects arising from the high value of the doping level lead to a strong variation of the pump power and signal gain along the fiber. We found that bidirectional pumping presents larger advancements than co-propagating and counter-propagating configurations. Numerical simulations allow us to explain the phenomenon in terms of the gain profile uniformity.

Keywords: Slow and fast light; coherent population oscillation; erbium-doped fiber.

1. Introduction

Great effort has focused in controlling the speed of light in solid state materials at room temperature due to the potential development of all-optical signal processing devices.^{1,2} To this aim, one of the most promising techniques is based on the coherent population oscillation (CPO) which produces a narrow spectral hole in the absorption or gain spectrum due to the periodic modulation of the ground state population at the beat frequency between a weak probe field and a strong control field sharing a common atomic transition.³ The first experiment concerning slow light propagation using CPO at room temperature was carried out by Bigelow *et al.* in a ruby rod.⁴ In addition, Bigelow *et al.*⁵ observed both superluminal and ultraslow light propagation in an alexandrite crystal arising from CPO involving chromium ions either in inversion or mirror sites within the crystal lattice. Room-temperature slow and fast light via CPO has also been observed in semiconductor structures, such as VCSELs⁶ and quantum dots,⁷ in solid state crystals,⁸ and in biological thin films.⁹

A modification of group velocity by CPO has been reported in an erbium doped fiber (EDF) by Schweinsberg *et al.*,¹⁰ where an amplitude-modulated 1550 nm

signal co-propagates with a 980 nm pump beam. They used a 13 m-long EDF with Er ion density of $1.78 \times 10^{24} \text{ m}^{-3}$ (90 ppm wt.). They observed a change from subluminal to superluminal propagation upon increasing pump power. One year before, experiments on slow and fast light in optical fibers were carried out by Song *et al.*¹¹ and Okawachi *et al.*¹² using another technique, stimulated Brillouin scattering (SBS). This method consists of the interaction of two propagating waves, a pump wave and a Stokes wave, which generates an acoustic wave at the frequency difference of the pump and the Stokes fields. The slow light resonance can be placed at the desired wavelength by changing the frequency of the pump field. Optical fibers are compatible with modern telecommunication systems, so these works represent a great step towards the development of all-optical signal processing devices.

Many applications concerning EDF amplifiers (EDFAs), such as high-speed optical communications, require high ion doping levels to minimize the fiber length. The effect of ion density on the slow light propagation enabled by CPO has been experimentally addressed for highly doped erbium fibers.^{13,14} It was found that ultra-high ion concentration (above 3000 ppm wt.) can simultaneously increase the fractional delay and the bandwidth of the signals that can propagate through the fibers without noticeable distortion. Furthermore, the effect of high doping levels in slow and fast light propagation in an EDFA in the forward pump mode was analyzed in Refs. 15 and 16. A change from subluminal to superluminal propagation solely upon increasing the beat frequency between the weak and the control fields was observed due to the interplay between strong pump depletion along the fiber and pump-power broadening of the transparency spectral hole induced by CPO.

It is well-known that pumping scheme in an EDFA is an important factor in determining its performance (gain and noise figure). In a co-pumped design, low gain is achieved in contrast to the counter-pumped design where the gain is relatively higher.^{17,18} As a compromise, bidirectional pumping scheme presents a gain between that of the unidirectional pumping schemes when using the same total pump power.¹⁹ In fact, gain and noise figure can be controlled by adjusting the pumping power ratio.

In this work, we analyze the influence of the pumping scheme on the superluminal propagation of amplitude-modulated signals through highly doped erbium fibers. As the signal gain depends on the pumping scheme, the advancement of the modulated signal when propagating along a highly doped erbium fiber is expected to depend on the pumping configuration. In fact, we will show how the bidirectional pumping scheme produces larger advancements than the unidirectional pumping schemes.

The paper is organized as follows. The theoretical model used to study coherent population oscillations in highly doped erbium fibers is described in Sec. 2 and is based on Ref. 20. In this model, the effects of ion pairs via inhomogeneous up-conversion processes are taken into account. It has been shown that this phenomenon is responsible for the gain degradation that appears in highly doped erbium fiber

amplifiers.^{21–23} The experimental setup is presented in Sec. 3 and the results and discussion in Sec. 4. The final conclusions are given in Sec. 5.

2. Model of Propagation Equations

The propagation of an amplitude periodically modulated signal through an erbium-doped material has been modeled in previous works on CPO by using both semi-classical and rate equation procedures.^{8,10} We consider the erbium ions as three-level atomic systems interacting with a power-modulated 1536 nm signal and a 977 nm pump. We assume a fast decay from the upper state pumped by the 977 nm laser which allows us to reduce the system to a two-level system [cf. Fig. 1(a)]. At high doping levels, as the one we are using here, previous works have shown deleterious effects on the output performance of high-concentration EDFAs due to inhomogeneous upconversion processes of ion pairs. In these processes, energy transfer takes place between two adjacent excited paired ions, i.e., one initially excited (${}^4I_{13/2}$) erbium ion (donor) donates its energy to its neighboring excited erbium ion (acceptor), producing one upconverted ion and one ground-state ion ${}^4I_{15/2}$. The upconverted ion then relaxes rapidly to the initial state ${}^4I_{13/2}$. As a result of this interaction, one excited ion is lost.

Following the model developed by Li *et al.*²⁰ to explain gain degradation in EDFAs due to inhomogeneous upconversion or pair-induced quenching (PIQ), we divide the erbium ions into two groups: isolated ions with an excited-state lifetime close to 10 ms and paired ions with a very fast decay of the pair excited-state (close to microseconds). The isolated ions can be described as a two-level system [cf. Fig. 1(a)], where N_1 and N_2 are the population densities of the ground state ${}^4I_{15/2}$ and the upper state ${}^4I_{13/2}$ normalized to the total ion density ρ , respectively. Then, the rate equation for N_1 is:

$$\frac{dN_1}{dt} = \frac{1 - 2k - N_1}{\tau} + \frac{P_s}{2\tau} (1 - 2k - 2N_1) - \frac{P_p^+ + P_p^-}{\tau} N_1, \quad (2.1)$$

where t is the time variable and $\tau = 10.5$ ms is the lifetime of the metastable state ${}^4I_{13/2}$. P_s is the signal power along the fiber normalized to the signal saturation

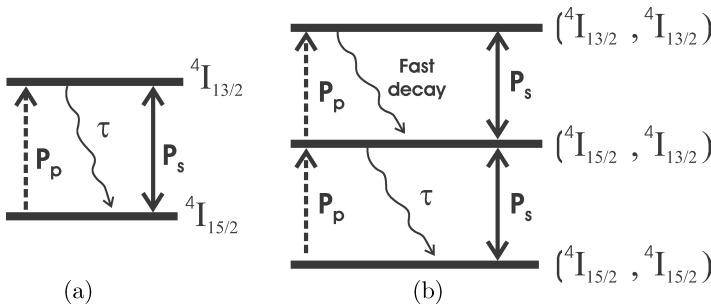


Fig. 1. (a) Two-level system for isolated Er ions and (b) three-level system for Er ion pairs. We also show the signal beam P_s and the total pump beam $P_p = P_p^+ + P_p^-$.

power $P_{ssat} \equiv \hbar\omega_s A_s / (\tau(\sigma_{21} + \sigma_{12}))$, where σ_{21} and σ_{12} are the emission and absorption cross sections, respectively, at the signal frequency ω_s , and A_s is the signal mode area. We assume equal cross sections, i.e., $\sigma_{21} \simeq \sigma_{12}$. P_p^+ and P_p^- are the forward and backward pump powers along the fiber normalized to the pump saturation power $P_{psat} \equiv \hbar\omega_p A_p / (\tau\sigma_{13})$, where σ_{13} is the absorption cross section at the pump frequency ω_p , and A_p is the pump mode area. k is the fraction of ion pairs in the total ion concentration ρ , then $N_1 + N_2 = 1 - 2k$.

The ion pairs can be described as a three-level system: the ground state (${}^4I_{15/2}, {}^4I_{15/2}$), the intermediate level (${}^4I_{15/2}, {}^4I_{13/2}$), and the upper level (${}^4I_{15/2}, {}^4I_{15/2}$) with normalized population densities N_{11} , N_{12} and N_{22} , respectively [cf. Fig. 1(b)]. For the sake of simplicity, and due to the fast decay of the upper level, we consider only the two lower levels, i.e., $N_{11} + N_{12} \simeq k$. Then, the rate equation for N_{11} is:

$$\frac{dN_{11}}{dt} = \frac{k - N_{11}}{\tau} + \frac{P_s}{2\tau} (k - 2N_{11}) - \frac{P_p^+ + P_p^-}{\tau} N_{11}. \quad (2.2)$$

The propagation equations for the signal power P_s , the forward pump power P_p^+ , and the backward pump power P_p^- along the fiber are:

$$\frac{dP_s}{dz} = \alpha_s (1 - 2k - 2N_1 - N_{11}) P_s, \quad (2.3)$$

$$\frac{dP_p^+}{dz} = -\alpha_p (N_1 + k) P_p^+, \quad (2.4)$$

$$\frac{dP_p^-}{dz} = \alpha_p (N_1 + k) P_p^-, \quad (2.5)$$

where $\alpha_s \equiv \sigma_{12}\rho\eta_s$ is the signal absorption coefficient, with $\eta_s = A_c/A_s$ the ratio between the fiber core area A_c and the signal mode area A_s , and $\alpha_p \equiv \sigma_{13}\rho\eta_p$ is the pump absorption coefficient, with $\eta_p = A_c/A_p$ the ratio between A_c and the pump mode area A_p . When we modulate the signal power as follows: $P_s = P_0 + P_m \cos(2\pi f_m t)$ (where P_0 is the normalized average signal power, P_m is the normalized modulation amplitude, and f_m is the modulation frequency), the ground state population of both isolated and paired ions will be forced to oscillate with the same frequency as $N_1 = N_{1st} + N_{1c} \cos(2\pi f_m t) + N_{1s} \sin(2\pi f_m t)$ and $N_{11} = N_{11st} + N_{11c} \cos(2\pi f_m t) + N_{11s} \sin(2\pi f_m t)$, respectively, where the steady state populations and the amplitude of the population oscillations can be obtained from Eqs. (2.1) and (2.2). Finally, we can obtain the propagation equations for the normalized average powers and the phase shift experienced by the periodic part of the signal ϕ , which measures the fractional delay or advancement $F \equiv \phi/(2\pi)$:

$$\frac{dP_0}{dz} = -\frac{\alpha_s P_0}{\omega_c} \left[(1 - 2k) (1 - P_p^+ - P_p^-) + k \left(1 + \frac{P_0}{2} \right) \right], \quad (2.6)$$

$$\frac{dP_p^+}{dz} = -\frac{\alpha_p P_p^+}{\omega_c} \left[1 + \frac{P_0}{2} + k (P_p^+ + P_p^- - 1) \right], \quad (2.7)$$

$$\frac{dP_p^-}{dz} = \frac{\alpha_p P_p^-}{\omega_c} \left[1 + \frac{P_0}{2} + k(P_p^+ + P_p^- - 1) \right], \quad (2.8)$$

$$\frac{d\phi}{dz} = \frac{\alpha_s P_0}{\omega_c} \frac{2\pi f_m \tau}{\omega_c^2 + (2\pi f_m \tau)^2} \left(1 - \frac{3k}{2} \right) (P_p^+ + P_p^- - 1), \quad (2.9)$$

where $\omega_c \equiv 1 + P_0 + P_p^+ + P_p^-$ is a dimensionless frequency that determines the width of the transparency hole created in the absorption or gain spectrum by means of CPO.¹

3. Experimental Setup

The experimental setup is depicted in Fig. 2 and consists of a 1 m-long EDF pumped with a 977 nm beam in three different pump configurations: forward pump mode, backward pump mode, and bidirectional pump mode (Fig. 2 shows the bidirectional pump configuration). The signal beam comes from a pigtailed distributed feedback laser diode operating at 1536 nm with a current and temperature controller that allows us to keep the laser at room temperature. The signal beam is split into two beams: one part of the beam (1%) is sent directly to a switchable-gain amplified InGaAs photodetector to be used as reference. The other part of the beam (99%) goes through the EDF and then to an identical photodetector. The EDF is pumped by means of a pigtailed distributed feedback laser diode operating at 977 nm provided also with a current and temperature controller. The signal and pump beams are injected into the EDF through two wavelength division multiplexers. Both, the reference and the EDF signals are recorded with a fast data acquisition card and then transferred to a computer for analysis. The experiment is controlled with a LabView program.

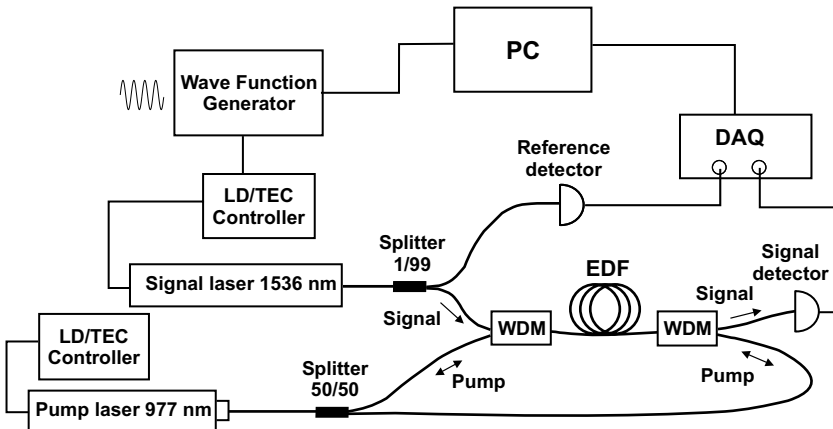


Fig. 2. Experimental setup used to measure slow and fast light in EDFs. LD/TEC, laser diode current and temperature controller; WDM, wavelength division multiplexer; EDF, erbium doped fiber; DAQ, data acquisition card; PC, personal computer.

We use a single mode Al_2SiO_5 -glass-based fiber highly doped with Er^{3+} ions with ion density $6.3 \times 10^{25} \text{ m}^{-3}$ (3150 ppm wt.). The fiber has a nominal mode field diameter at 1550 nm of $6.5 \mu\text{m}$, a fiber cladding of $245 \mu\text{m}$, and a numerical aperture of 0.2. By using typical values for the parameters from previous works^{13, 15} we obtain the linear absorption coefficient of the signal $\alpha_s \simeq 0.15 \text{ cm}^{-1}$ (optical density $\alpha_s L \simeq 15$ where L is the fiber length) and the pump $\alpha_p \simeq 0.13 \text{ cm}^{-1}$ (optical density $\alpha_p L \simeq 13$) and the saturation power of the signal $P_{ssat} \simeq 0.4 \text{ mW}$ and the pump $P_{psat} \simeq 1.3 \text{ mW}$. We use a fraction of ion pairs of $k = 0.2$ which is the value estimated in Ref. 24 for the doping level we are using in this work.

The injection current of the laser signal is sinusoidally modulated by a function generator so that the signal power injected into the fiber is $P_s = P_0 + P_m \cos(2\pi f_m t)$. In what follows, we use an average signal power of 0.5 mW , very close to the signal saturation power, and we keep the ratio $P_m/P_0 \simeq 0.5$. Previous works of CPO in EDFs have shown that the delay is not affected while varying this ratio between very low values up to 0.7.¹³ This is in agreement with the theoretical model described above which has been derived by using a perturbation method. We compute the time delay or advancement t_d from the correlation of the reference signal and the signal propagated through the EDF. The fractional delay or advancement is defined as $F = t_d f_m$, i.e., the time delay normalized to the period of the modulated signal.

In order to study the effect of pump configuration, we measure the time delay or advancement by injecting into the EDF the same total power $P_p^{(in)} = P_p^+(z=0) + P_p^-(z=L)$ for the three pump modes. In the bidirectional case, we inject half of the total pump power for each fiber end, i.e., $P_p^+(z=0) = P_p^-(z=L) = P_p^{(in)}/2$.

4. Results and Discussion

4.1. Maximum fractional advancement

We measure the fractional advancement F versus the modulation frequency f_m for several pump powers, P_p . The three pump configurations present the same general trend. As an example, Fig. 3 shows the results obtained for the bidirectional pump configuration. At low pump levels, delay is achieved for all the values of f_m (see for example the lowest curve represented on Fig. 3 which corresponds to a pump power of 7 mW) whereas at high pump levels, advancement is achieved for all modulation frequencies (see the highest curve corresponding to a pump power of 105 mW). This transition from subluminal to superluminal propagation upon an increase in pump power is associated to a transition from signal absorption to signal gain. Moreover, for high pump values the increase of pump power results in a roughly linear increase in the optimum frequency (i.e., the modulation frequency at which the maximum advancement occurs). At moderate pump powers, a net delay or advancement is obtained depending on the value of f_m (see curve with open symbols in Fig. 3 which corresponds to a pump power of 20 mW). This behavior is due to the interplay between the strong pump absorption and the pump-power broadening of the spectral hole induced by CPO. Thus, high-frequency modulated

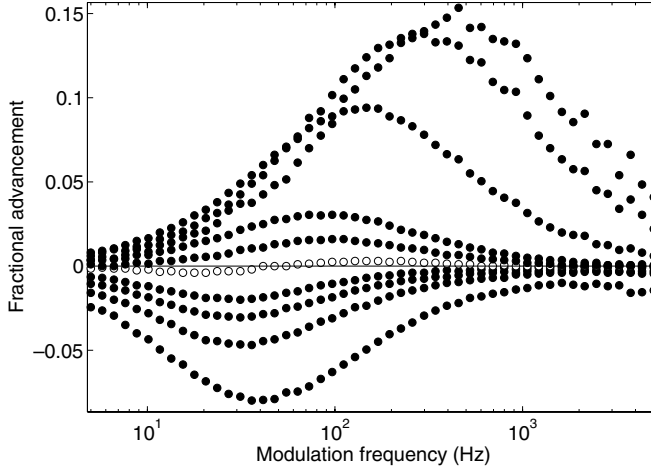


Fig. 3. Experimental fractional advancement F versus modulation frequency f_m for the bidirectional pump configuration and for several values of the total pump power ranging from 7 mW (delay $F < 0$) to 105 mW (advancement $F > 0$). Open symbols curve corresponds to a pump power of 20 mW.

signals suffer strong advancement along the fiber region where gain is achieved and there is slight delay along the rest of the fiber length so net advancement of these high-frequency signals is achieved at the output of the fiber. The opposite situation occurs for low frequency modulated signals, leading to net delay. By comparing the three pump configurations, we find that the range of pump powers that leads to this peculiar behavior, i.e., a delay section for low-modulation-frequency signals and an advancement section for high-modulation-frequency signals, is strongly reduced in the bidirectional configuration. In particular, we obtain a range of pump powers of 24 mW, 11 mW and 3 mW for forward, backward and bidirectional configurations, respectively. This reduction could be related to the higher uniformity of the gain spatial profile along the fiber obtained by the bidirectional pumping.

For a more quantitative comparison among the different pump configurations, we plot in Fig. 4 the experimental (a) and simulated (b) maximum fractional advancement or delay as a function of the total pump power. The simulated results were calculated by numerically solving Eqs. (2.6)–(2.9) using a fourth-order Runge-Kutta shooting method. Note that the bidirectional pumping allows larger advancement values than the forward and backward configurations. These two last pump configurations present similar values. We also plot in Fig. 4 the experimental (c) and simulated (d) frequency where the maximum fractional advancement occurs (i.e., optimum frequency) versus the total pump power. For simplicity, we have not included the values of the frequencies at which maximum fractional delay occurs. We can observe a similar behavior for the optimum frequency for the three pump configurations. Excluding some differences in the low power region, the optimum frequency linearly increases with pump power, which points out that the transparency

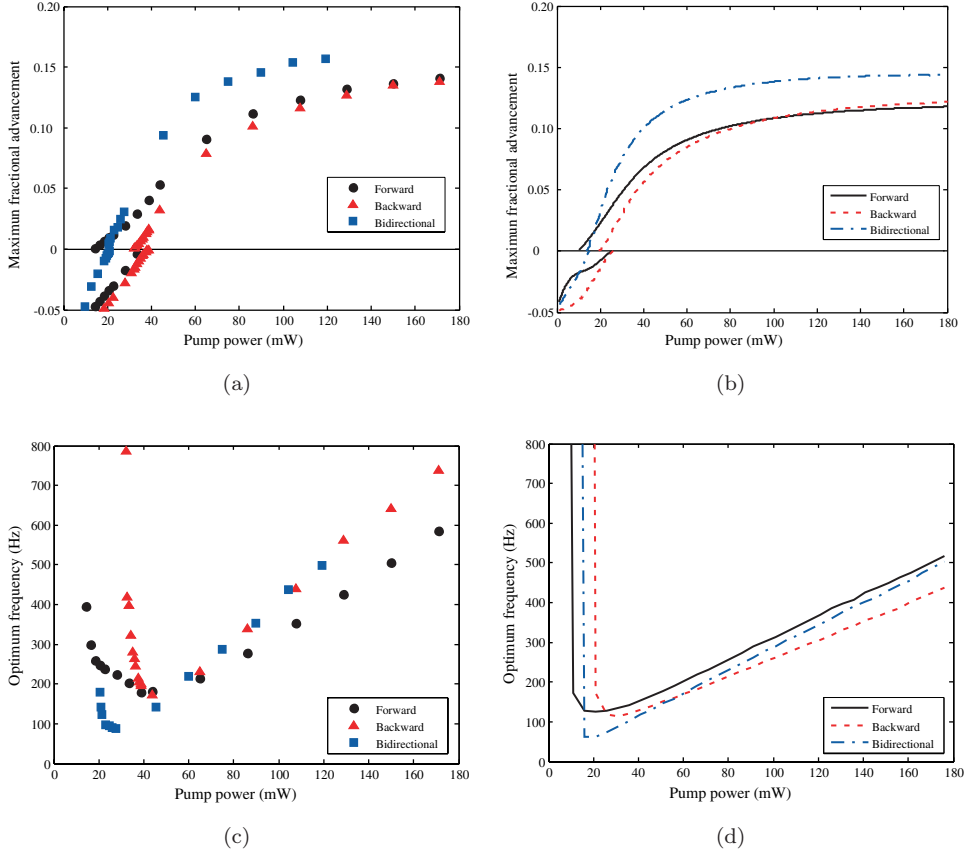


Fig. 4. Experimental (a) and simulated (b) maximum fractional advancement and delay versus total pump power for three pump configurations. Experimental (c) and simulated (d) optimum frequency versus total pump power for three pump configurations.

spectral hole is power broadened. The simulations agree with the experimental findings (cf. Figs. 4(b) and 4(d)). In conclusion, we have found that the pump configuration plays an important role in the advancement of light signals, whereas the bandwidth of the signals remains unaltered.

To better understand the origin of the fast light enhancement obtained by bidirectional pumping, let us study the signal gain of the EDFA. To this end, we measure the net gain of the EDFA when a continuous wave signal propagates through a 1 m-long fiber while pumping it in the three pump configurations described above. The results are plotted in Fig. 5 showing that the highest net gain takes place for the backward pumping configuration (in agreement with other works^{17–19}) whereas the forward pump shows the lowest net gain. This result does not allow us to properly explain that the largest advancement occurs in the bidirectional scheme, as shown in Fig. 4. However, as the advancement of the modulated signals accumulates as the signals propagate along the fiber, the spatial variation of the signal

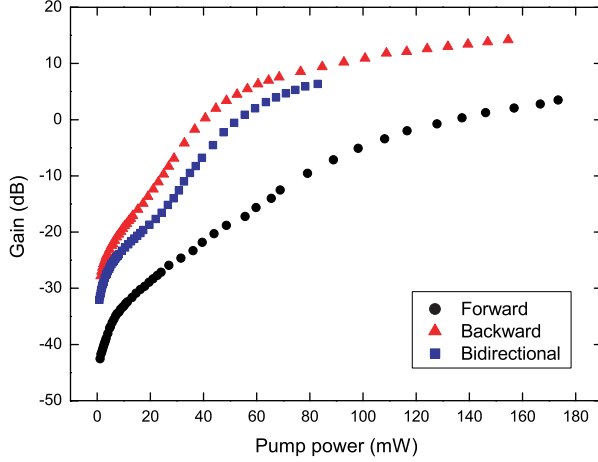


Fig. 5. Experimental gain of a continuous wave 1536 nm-signal versus total pump power for the three different pump configurations.

gain along the fiber could explain the fast light enhancement obtained by bidirectional pump. With this aim, we have analyzed the spatial variation of the signal and pump powers along the fiber length. We plot in Fig. 6 the simulated pump (a) and signal (b) powers as a function of the distance along the fiber for the three pumping schemes. The forward pump configuration leads to a strong signal gain in the front part of the fiber. However, signal absorption occurs at the end of the fiber which reduces the growth of the advancement that was achieved in the first part of the fiber. The backward pump configuration does not produce signal gain in the front part of the fiber although a very rapid increase of the signal value is carried out at the end of the fiber. The bidirectional scheme presents a more uniform pump spatial profile which allows a continuous increase of the signal all along the fiber length. Although the net signal gain at the fiber output in the bidirectional scheme is slightly lower than the net gain in the backward case, the continuous growth of the gain in the bidirectional scheme leads to the largest value of the advancement at the fiber end. From Eq. (2.9) it can be easily obtained that the maximum advancement is achieved at high values (above the saturation value) of the pump and signal powers for the optimum modulation frequency $f_m \simeq \omega_c / (2\pi\tau)$. Figure 6 shows that bidirectional pumping maintains higher signal and pump values during longer distances compared to the signal and pump values in the backward pumping due to the uniformity of the pump profile.

4.2. Effect of fiber length on fast light propagation

As we have shown, the spatial profiles developed by the pump and signal powers govern the behavior of the fractional advancement. Therefore, we study how the previous results (which were obtained when using a 1 m-long fiber) depend on the

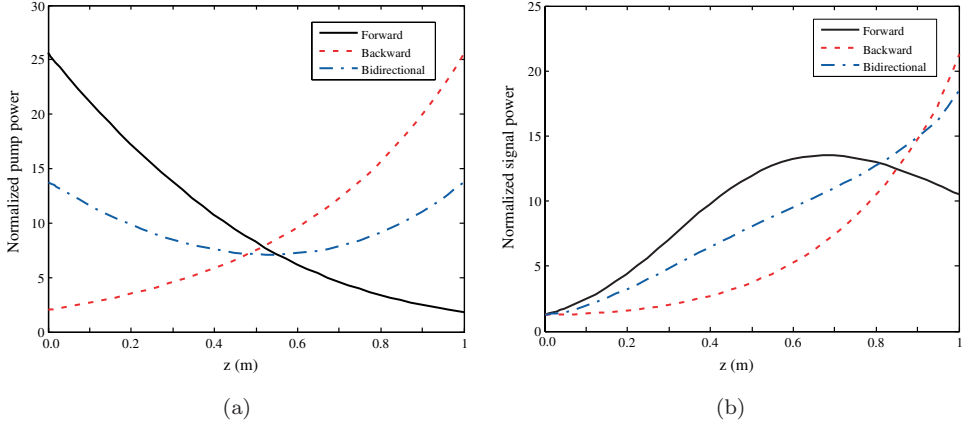


Fig. 6. Simulated normalized total pump power $P_p = P_p^+ + P_p^-$ (a) and average signal power P_0 (b) versus the distance along the fiber length z for the three pumping schemes. The injected pump power is 100 mW.

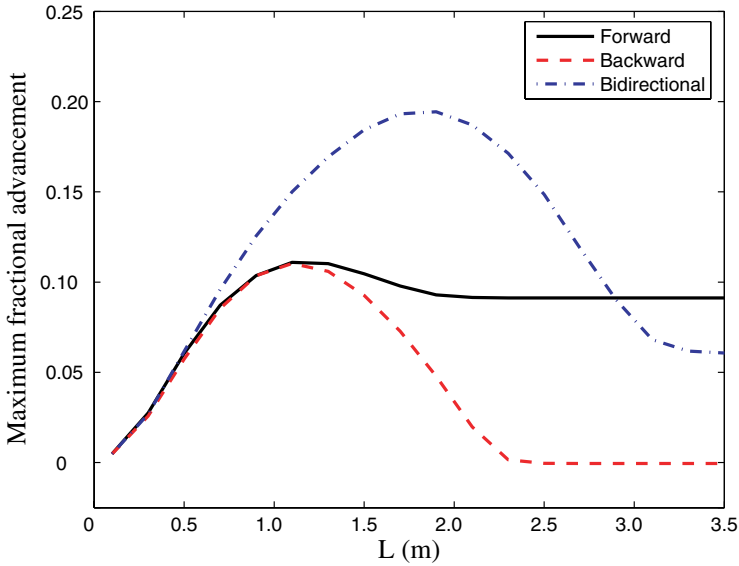


Fig. 7. Maximum fractional advancement versus fiber length L for a pump power of 100 mW and for the three different pump configurations.

fiber length. To this end, we numerically analyze the behavior of the maximum fractional advancement (with respect to f_m) as a function of the fiber length for the three pumping schemes and using an injected total pump power of 100 mW. The simulated curves are plotted in Fig. 7. We observe that for very short fiber lengths (up to ≈ 0.5 m), the advancement does not depend on the pumping configuration since all pumps lead to similar gain spatial profiles. However, as we increase

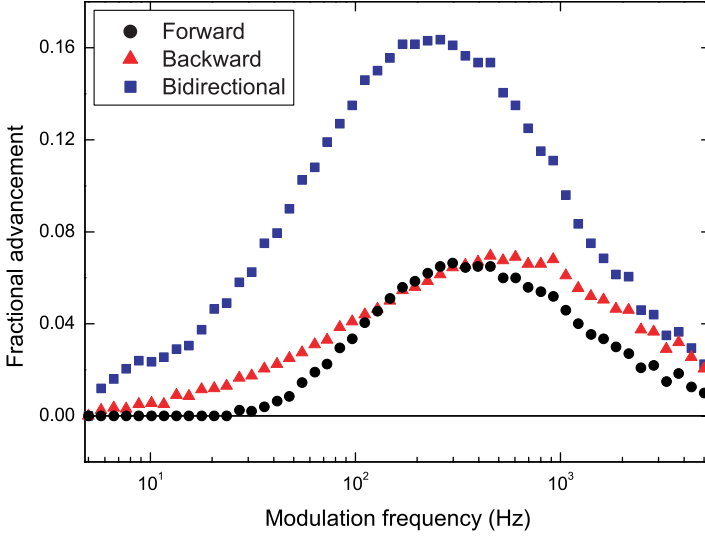


Fig. 8. Experimental fractional advancement F versus modulation frequency f_m for the three different pump configurations, for a pump power of 100 mW, and a fiber length of 1.5 meters.

the fiber length up to 2 m, the bidirectional pumping gives larger advancements than the other configurations, in agreement with the results shown in the previous subsection. Thus, Fig. 7 predicts that, for this pump value, the maximum advancement is achieved for the bidirectional pumping, being the optimum fiber length around 1.8m. In order to experimentally observe this result, we have measured the fractional advancement as a function of the modulation frequency f_m for the three pump configurations using a 1.5 m-long fiber. The results are shown in Fig. 8, which shows that much larger advancements are achieved at bidirectional pumping. If we keep increasing the fiber length above 3 m, the counter-propagating pump is not able to produce any significant advancement since the signal power falls down to almost zero before being amplified by the counter-propagating pump. In this extreme situation, that is, for high optical densities ($\alpha_s L \simeq 52.5$ and $\alpha_p L \simeq 45.5$), the advancement is only accumulated on the first part of the fiber, where a non-negligible signal power is being amplified by the co-propagating pump. That is the reason why for very long fiber lengths the forward scheme produces larger advancements than the bidirectional one (as can be seen in Fig. 7).

5. Conclusion

We have studied the role of the pumping scheme on the propagation velocity of amplitude-modulated signals through highly doped erbium fibers based on coherent population oscillations. It is well-known that pumping scheme in EDFAs plays an important role in the signal gain. We have found that the pump configuration strongly affects the group velocity of light signals whereas the bandwidth of the

signals remains unaltered. In particular, bidirectional pumping scheme produces larger advancements than the unidirectional pumping schemes. However, the highest net signal gain is obtained by backward pumping. Numerical simulations allow us to obtain that bidirectional pumping presents more uniform spatial profiles for the pump and signal powers which could explain the fast light enhancement. Moreover, we have found an optimum fiber length at which the fractional advancement is maximum for each pumping scheme.

Acknowledgments

This work has been supported by Projects no. PR34/07-15847, FIS2007-65382, CCG07-UCM/ESP-2179 and CCG08-UCM/ESP-4220 from Spain.

References

1. R. W. Boyd, D. J. Gauthier and A. L. Gaeta, *Opt. Photon. News* **17** (2006) 18–23.
2. R. W. Boyd and P. Narum, *J. Modern Opt.* **54** (2007) 2403–2411.
3. L. W. Hillman, R. W. Boyd, J. Kransinski and C. R. Stroud, *Opt. Commun.* **45** (1983) 416–419.
4. M. S. Bigelow, N. N. Lepeshkin and R. W. Boyd, *Phys. Rev. Lett.* **90** (2003) 113903.
5. M. S. Bigelow, N. N. Lepeshkin and R. W. Boyd, *Science* **301** (2003) 200–202.
6. X. Zhao, P. Palinguinis, B. Pesala, C. J. Chang-Hasnain and P. Hemmer, *Opt. Express* **13** (2005) 7899–7904.
7. H. Su and S. L. Chuang, *Opt. Lett.* **31** (2006) 271–273.
8. E. Baldit, K. Bencheikh, P. Monnier, J. A. Levenson and V. Rouget, *Phys. Rev. Lett.* **95** (2005) 143601.
9. P. Wu and D. V. Rao, *Phys. Rev. Lett.* **95** (2005) 253601.
10. A. Schweinsberg, N. N. Lepeshkin, M. S. Bigelow, R. W. Boyd and S. Jarabo, *Europhys. Lett.* **73** (2006) 218–224.
11. K. Y. Song, M. G. Herráez and L. Thèvenaz, *Opt. Express* **13** (2005) 82–88.
12. Y. Okawachi, M. S. Bigelow, J. E. Sharping, Z. Zhu, A. Schweinsberg, D. J. Gauthier, R. W. Boyd and A. L. Gaeta, *Phys. Rev. Lett.* **94** (2005) 153902.
13. S. Melle, O. G. Calderón, F. Carreño, E. Cabrera, M. A. Antón and S. Jarabo, *Opt. Commun.* **279** (2007) 53–63.
14. Y. Zhang, W. Qiu, J. Ye, N. Wang, J. Wang, H. Tian and P. Yuan, *Opt. Commun.* **281** (2008) 2633–2637.
15. S. Melle, O. G. Calderón, C. E. Caro, E. Cabrera-Granado, M. A. Antón and F. Carreño, *Opt. Lett.* **33** (2008) 827–829.
16. O. G. Calderón, S. Melle, M. A. Antón, F. Carreño, F. Arrieta-Yañez and E. Cabrera-Granado, *Phys. Rev. A* **78** (2008) 053812.
17. S. Milo, R. F. Souza, M. B. C. Silva, E. Conforti and A. C. Bordonalli, An EDFA Theoretical Analysis Considering Different Configurations and Pumping Wavelengths, in *Proc. International Microwave and Optoelectronics Conference, IMOC* (2003), pp. 105–110.
18. V. Sinivasagam, M. A. G. Abushagur, K. Dimiyati and F. Tumiran, *IEICE Electronics Express* **2** (2005) 154–158.
19. R. Deepa and R. Vijaya, *Optical Fiber Technology* **14** (2008) 20–26.
20. J. Li, K. Duan, Y. Wang, W. Zhao, J. Zhu, Y. Guo and X. Lin, *J. Modern Opt.* **55** (2008) 447–458.

21. F. Sanchez, P. L. Boudec, P.-L. Francois and G. Stephan, *Phys. Rev. A* **48** (1993) 2220–2229.
22. J. L. Wagener, P. F. Wysocki, M. J. F. Digonnet, H. J. Shaw and D. J. DiGiovanni, *Opt. Lett.* **18** (1993) 2014–2016.
23. P. F. Wysocki, J. L. Wagener, M. J. F. Digonnet and H. J. Shaw, Evidence and modeling of paired ions and other loss mechanisms in erbium-doped silica fibers, in *Proc. Fiber Laser Source and Amplifiers IV. SPIE 1789* (1993), pp. 66–79.
24. O. G. Calderón, S. Melle, F. Arrieta-Yañez, M. A. Anton and F. Carreño, *J. Opt. Soc. Am. B* **25** (2008) C55–C60.